CONF-881275--1

[To be published in *Zinc Oxide Varistors: Science and Technology*, American Ceramic Society Conference Proceedings]

CONF-881275--1

DE89 008234

ZINC OXIDE VARISTOR TIME RESPONSE

F. A. Modine, R. W. Major, S.-I. Choi, L. B. Bergman, and M. N. Silver

"The submitted manuscript has been authored by a contractor of the U.S. Government under contract No. DE-AC05-84OR21400. Accordingly, the U.S. Government retains a nonexclusive, royalty-free license to publish or reproduce the published form of this contribution, or allow others to do so, for U.S. Government purposes."

SOLID STATE DIVISION
OAK RIDGE NATIONAL LABORATORY
Oak Ridge, Tennessee 37831-6030
operated by
MARTIN MARIETTA ENERGY SYSTEMS, INC.
for the
U.S. DEPARTMENT OF ENERGY
under contract DE-AC05-84OR21400

MASTER

[February 1989]

ZINC OXIDE VARISTOR TIME RESPONSE*

F. A. Modine and R. W. Major†
Solid State Division
Oak Ridge National Laboratory
Oak Ridge, TN 37831-6030

S.-I. Choi, L. B. Bergman, and M. N. Silver
University of North Carolina
Chapel Hill, NC 27514

ABSTRACT

The application of a voltage to a zinc oxide varistor produces transient currents that persist on a time scale extending from 10^{-8} to 10^{5} seconds at the least. The transient currents are characterized by a power-law time dependence (i.e., $I = I_o/t^m$, where m is a little less than unity) and a weak temperature dependence that is described by a thermal activation energy of about 100 meV or less. The time dependence is confirmed by an ac admittance that increases as a non-integer power of the frequency [i.e., $Y = K(j\omega)^m$], with Fourier theory providing the connection between the time and frequency measurements. Also, the transient currents are accompanied by changes in the ac admittance measured at fixed frequencies that reveal similar time and temperature dependencies. The transient currents are not well understood, but they are typical of the non-Debye electrical response that is found in many materials. An explanation of the transients is obtained if a distribution of relaxation times is assumed.

I. INTRODUCTION

Many varistor publications are concerned with electrical conduction at high applied voltages (i.e., above breakdown voltage) and short times (e.g., fast pulse response). Less attention has been given to the small currents generated by applied voltages less than the breakdown threshold, which are the subject of this article. However, Philipp and Levinson[1] have studied the subject. The currents consist primarily of slowly changing polarization currents that are characterized by a power-law rather than an exponential time dependence. Because of these currents, it may take many minutes, hours, or even days before varistor conduction reaches a steady state. The currents represent a non-Debye electrical response that has been observed in materials other than varistors. Review articles[2,3] treat the general subject and provide many examples. Even though there is considerable interest in the phenomenon, it is poorly understood and has not been generally recognized as an important aspect of varistor conduction. Nevertheless, polarization currents influence many aspects of varistor conduction, and it is necessary to recognize and account for these currents in order to measure and interpret varistor properties correctly. Moreover, these low-level polarization currents are of practical importance. They contribute power dissipation which adversely affect a varistor's stability against thermal runaway. Finally, the varistor time response provides a test of theoretical models, but it is complicated by the non-Debye response.

II. EXPERIMENTAL PROCEDURES

Measurements were made on commercial low- and medium-voltage varistors (GE V12ZA1 and GE V130L20). The characteristics of these types differ and to a lesser extent varistors of the same type have varying characteristics. In general, the same varistor was used for all the measurements of a particular figure, but different varistors were used for different sets of measurements.

The transient polarization currents were measured by the method of Philipp and Levinson,[1] except that a Kepco model OPS 1000 B programmable power supply replaced the battery and a Hewlett-Packard model 3455 A digital voltmeter and a Hewlett-Packard model 9825 computer replaced the recorder. The computer acquired current measurements on a logarithmic time base. Temperature was controlled with a cold-gas-flow system.

Admittance measurements were made with a Hewlett-Packard model 4192 impedance analyzer that was operated in the resistor-parallel-to-a-capacitor mode of analysis. The instrument has a built-in dc bias voltage, and it was interfaced to a Hewlett-Packard model 236 computer, which was used for data acquisition and analysis. The temperature was controlled with a Lake Shore Cryotronics model DTC-500 controller.

III. TRANSIENT POLARIZATION CURRENTS

Figure 1 shows charging currents in medium voltage varistors. Polarization currents dominate initially, but the polarization currents decay and steady-state conduction is evident at long times. The data confirm results of Philipp and Levinson[1] and in addition illustrate the voltage dependence of the phenomena. Both the polarization and steady-state currents exhibit a linear response to applied voltages that are less than one-third of the breakdown voltage of about 200 V, but at higher voltages nonlinearity becomes evident even in the polarization current. At room temperature and low voltages, about 10^3 seconds is required for the polarization currents to become negligible in comparison to the steady-state conduction. The polarization currents are predominant for longer times at low temperatures, because the thermally activated steady-state conduction is diminished. The measurement of steady-state current-voltage characteristics becomes a test of patience at low voltages and low temperatures.

Figure 2 shows the discharge currents that follow the removal of an applied voltage. At shorter times than 0.1 seconds, the varistor capacitance discharges at an exponential rate established by the RC time constant of the circuit,[4] but the figure reveals only a current that decreases almost inversely with time. The discharge currents are roughly described by the power law

$$I = I_o/t^m \ , \tag{1}$$

where m is less than unity. However, this law cannot be obeyed at either short or long times because the stored charge is finite, and the integral of the current must , therefore, converge. The slopes of the curves do increase in magnitude at times greater than 100 seconds. Between 0.1 and 100 s the curves are nearly straight but their slopes increase from about 0.8 to almost 1 as the voltage increases from 5 to 80 V, which indicates that highly-charged varistors discharge faster.

The discharge currents exhibit a temperature dependence as well as a time dependence. The inset of Fig. 2 is an Arrhenius plot of the temperature dependence of the current measured at fixed times after removing the applied voltage. The curves are fits to the data of the function

$$I(t = t_o) = I_1 \exp(-E_1 / k_B T) + I_2 \exp(-E_2 / k_B T) \ , \tag{2}$$

where I_1 and I_2 are time dependent. The results imply two processes with activation energies of about 160 meV and 10 meV. The higher energy is close to the 170 meV observed in deep level transient spectroscopy and can be interpreted as thermal emission from a deep level.[5] However, 10 meV is too low an energy to be interpreted in terms of thermal emission because the current persists too long.

Philipp and Levinson interpret the temperature dependence of the polarization currents in medium voltage GE varistors in terms of a single 35 meV activation energy.[1] However, the data of Fig. 2 cannot be so interpreted. We conclude that an Arrhenius plot of the data of Philipp and Levinson is consistent with a change of slope, but there are too few data points to identify two distinct slopes. In fact, if the data points between room and liquid nitrogen temperature are neglected in the inset of Fig. 2, a single activation energy of 34 ± 3 meV provides a reasonably good fit to the remaining data. This value is in remarkably good agreement with the 35 meV inferred by Philipp and Levinson from similar data.

Evidence that a voltage change induces a power-law time response in the varistor current for $10^{-7} \le t \le 10^{-3}$ s is provided by Fig. 3, which shows the current decay after a voltage pulse is applied. A pulse voltage below breakdown was employed. Initially, the discharge exhibits the exponential time dependence expected of a circuit with an RC time constant of about 10^{-7} seconds. Evidence of exponential time dependence can be seen in Fig. 3 for $t < 10^{-6}$ s. After the initial discharge of the varistor capacitance, the current exhibits a t^{-m} power-law decay with m close to unity. Once again a weak temperature dependence is found. An Arrhenius plot of the current measured at fixed times is inset in Fig. 3. To the extent that an activation energy can be identified from the plot, a value of about 38 meV is obtained.

IV. FREQUENCY RESPONSE

The frequency dependence of the varistor admittance can be used to verify and to extend the time-domain results. Fourier theory relates the time response of a varistor to its frequency response. The admittance as a function of frequency is the ratio of the Fourier transforms of current and voltage that are measured as a function of time. Assuming that a step change in the voltage induces a current that decreases inversely with time (see Eq. 1), the admittance is

$$Y(\omega) = I(\omega) / V(\omega) = (I_0 / V_0)\ \Gamma(1-m)(j\omega)^m = K(j\omega)^m \quad , \qquad (3)$$

where $j = (-1)^{1/2}$, V_0 is the magnitude of the voltage step, $\Gamma(1 - m)$ is the gamma function of argument (1 - m), and K is a constant that would simply be the capacitance if m = 1. In actuality m is a little less than unity, and

$$Y = G + j\omega C = K\ \omega^m [\cos(\pi m / 2) + j\ \sin(\pi\ m / 2)] \ . \qquad (4)$$

Consequently, the conductance G and the susceptance ωC exhibit the same power- law frequency dependence and, therefore, have a constant ratio. Figure 4 illustrates that this frequency dependence is measured in ZnO varistors. The slope of the curve is $m \approx 0.93$, which is in good agreement with the time-domain results. The results reveal a constant phase shift δ of the current relative to the voltage,

$$\delta = m\,\pi / 2 = \tan^{-1}(\omega C / G) = \tan^{-1}(1 / D) \quad . \qquad (5)$$

The behavior is characterized by a dissipation D that is almost frequency independent. The harmonic response of varistors has been studied by others.[6,7] However, while the connection between the time response and the frequency response is well known, the connection has not been emphasized for varistors. The frequency response verifies that the t^{-m} power law for the current holds for $10^{-8} < t < 10^{-2}$ s, and it extends beyond this range.

V. TRANSIENT AC ADMITTANCE

A different insight is obtained when the admittance at a fixed frequency is monitored as a function of time during the charging or discharging of the varistor. Figure 5 shows transient changes in the capacitance C and dissipation factor $D = G/\omega C$ that accompany the discharge of a varistor. The changes in C

and D with time and temperature are similar to the changes seen in the polarization currents.
A connection between the polarization current and the transient capacitance is provided by

$$I = V_0\, dC / dt = V_0\, C[d(\ln \varepsilon) / dt - d(\ln w) / dt] \qquad (6)$$

where ε and w are the dielectric function and the width, respectively, of the depletion region. The equation recognizes that both the dielectric function and the width of a grain boundary barrier device can change. Figure 6 shows plots of the derivatives of C and G with respect to time. The plots exhibit a time and temperature dependence which is nearly identical to that of the polarization current. The capacitance exhibits a power-law time dependence instead of the exponential time dependence that is commonly assumed when the deep-level transient spectra of varistors are interpreted.

A connection between the transient changes in C and G has already been established by Eq (4). However, note that the dissipation factor is not quite constant and that over-barrier conduction can also contribute.

$$G = \omega CD + \beta J_0 \exp(-\beta V_b), \qquad (7)$$

where $\beta = e/k_BT$, $J_o = AT^2$, k_B is the Boltzmann constant, A is the Richardson constant, and V_b is the barrier height. The first term of Eq. (7) follows from Eqs. (4) and (5), and the second term is the over-barrier contribution. The inset of Fig. 6 shows that the induced changes in C and G are directly proportional and only weakly temperature dependent. The slope of the curves is not much greater than unity and it decreases with increasing temperature. This suggests that the over-barrier conduction is negligible in these measurements.

VI. THEORETICAL INTERPRETATION

The non-Debye response of materials can be attributed to a distribution of Debye relaxations with different time constants.[2,3] The relaxations can be associated with either the reorientation of dipoles or the dynamics of charge trapping.[2,3] Application of a voltage to a distribution of Debye relaxations induces a current that is a superposition of exponential decays,

$$I = C_0 V_0 d\varepsilon / dt = C_0 V_0 (\varepsilon_s - \varepsilon_\infty) \int G(\tau) [\exp(-t/\tau)/\tau] d\tau, \qquad (8)$$

where C_o is the geometric capacitance in the absence of a dielectric, ε_s and ε_∞ refer to the static and high-frequency dielectric functions, and G(τ) is a distribution of relaxation times. A suitable distribution of relaxation times is obtained if the time constant is thermally activated,

$$\tau = \tau_o \exp(E / k_B T), \quad (9)$$

and a uniform distribution of activation energies is assumed.

$$G(\tau) = N(E)\, dE / d\tau = (E_{max} - E_{min})^{-1}\, k_B T / \tau, \quad (10)$$

where E_{max} - E_{min} is width of the distribution. From Eqs. (8) and (10),

$$I = C_o V_o[(\varepsilon_s - \varepsilon_\infty) / (E_{max} - E_{min})]\, k_B T / t \quad , \quad (11)$$

for $\tau_{min} < t < \tau_{max}$. Thus, a weak temperature dependence and an approximately correct time dependence can be obtained.

A power-law time dependence follows from a distribution of relaxation times that varies as τ^{-1}. This distribution is often an ad hoc assumption, but a similar distribution can be derived if the current is associated with tunneling from deep traps in the depletion region. The tunneling is initiated when the applied potential changes the Fermi level to give a metastable distribution of trapped charge. A WKB calculation of the tunneling induced by a constant potential gradient gives

$$\tau = \tau_o \exp(\gamma\, E_t^{3/2} / \mathcal{E}), \quad (12)$$

where $\gamma = 4(2m)^{1/2}/3\hbar e$, E_t is the trap depth and $\mathcal{E}$ is the field strength. For a parabolic potential barrier,

$$\mathcal{E} = (2V_b / x_o)\,(1 - x / x_o) \quad (13)$$

where V_b is the barrier height, x_o is the position of the depletion-layer edge, and x is distance. If a uniform spacial distribution of monoenergetic traps is assumed, Eqs. (12) and (13) yield the distribution

$$G(\tau) = N(x) dx / d\tau \sim 1 / [\ln(\tau / \tau_o)]^2 \tau \sim 1 / \tau \quad . \quad (14)$$

Hence, tunneling from deep traps could explain the power-law time dependence of the current and its weak temperature dependence as well.

*Research sponsored by the U.S. Department of Energy, Office of Energy Storage and Distribution under contract DE-AC05-84OR21400 with Martin Marietta Energy Systems, Inc., and by the Army Research Office under contract D AAL 03-88-K-0028.

†Permanent address: Department of Physics, University of Richmond, Richmond, VA 23173.

REFERENCES

1. H. R. Philipp and L. M. Levinson, *J. Appl. Phys.* **47**, 3177 (1976).
2. A. K. Jonscher, *Dielectric Relaxation in Solids*, (Chelsea Dielectrics Press, London, 1983).
3. D. M. Smyth, in *Oxides and Oxide Films*, ed. by J. W. Diggle (Marcel Dekker, New York, 1973).
4. F. A. Modine and R. B. Wheeler, *J. Appl. Phys.* **61**, 3093 (1987).
5. J. F. Cordaro, Y. Shim, and J. E. May, *J. Appl. Phys.* **60**, 4186 (1986).
6. L. M. Levinson and H. R. Philipp, *J. Appl. Phys.* **47**, 1117 (1976).
7. M. A. Alim, M. A. Seitz, and R. W. Hirthe, *J. Appl. Phys.* **63**, 2337 (1988).

FIGURE CAPTIONS

Fig. 1. Currents induced in a medium-voltage varistor by voltages that differ by multiples of 2. Solid line: 295 K; dashed line: 77 K.

Fig. 2. Discharge current transients induced in a medium-voltage varistor at 295 K by removal of voltages that differ by factors of 2. Inset is an Arrhenius plot of the current measured at 0.1, 1, and 10 s.

Fig. 3. Discharge current transients that follow application of a voltage pulse to a low-voltage varistor at 295 and 420 K. The inset is an Arrhenius plot of the current measured at 3×10^{-4} and 4×10^{-5} s after the pulse.

Fig. 4. Conductance and susceptance versus frequency for a low-voltage varistor at 295 K.

Fig. 5. Transients induced in the capacitance and dissipation factor of a low-voltage varistor measured at 10 kHz after removing a 10 V bias.

Fig. 6. Transients induced in the 10 kHz capacitance and conductance of a low-voltage varistor at 295 K by removing a potential of 10 V. The C_i and G_i denote initial values. The change in conductance versus the change in capacitance at 3 temperatures is plotted in the inset.

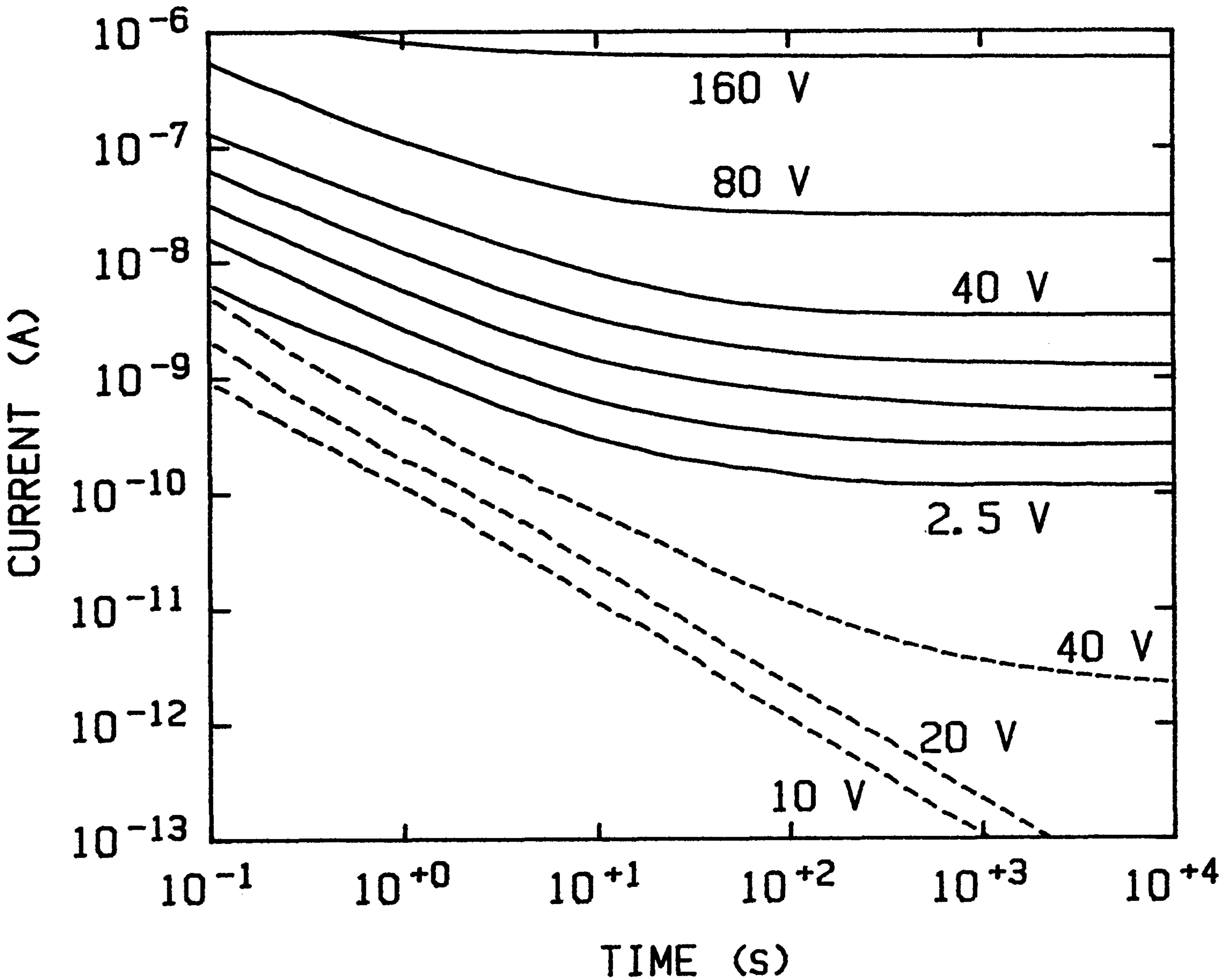

CURRENT (A)
10^-6
10^-7
10^-8
10^-9
10^-10
10^-11
10^-12
10^-13
160 V
80 V
40 V
2.5 V
40 V
20 V
10 V
10^-1
10^+0
10^+1
10^+2
10^+3
10^+4
TIME (s)

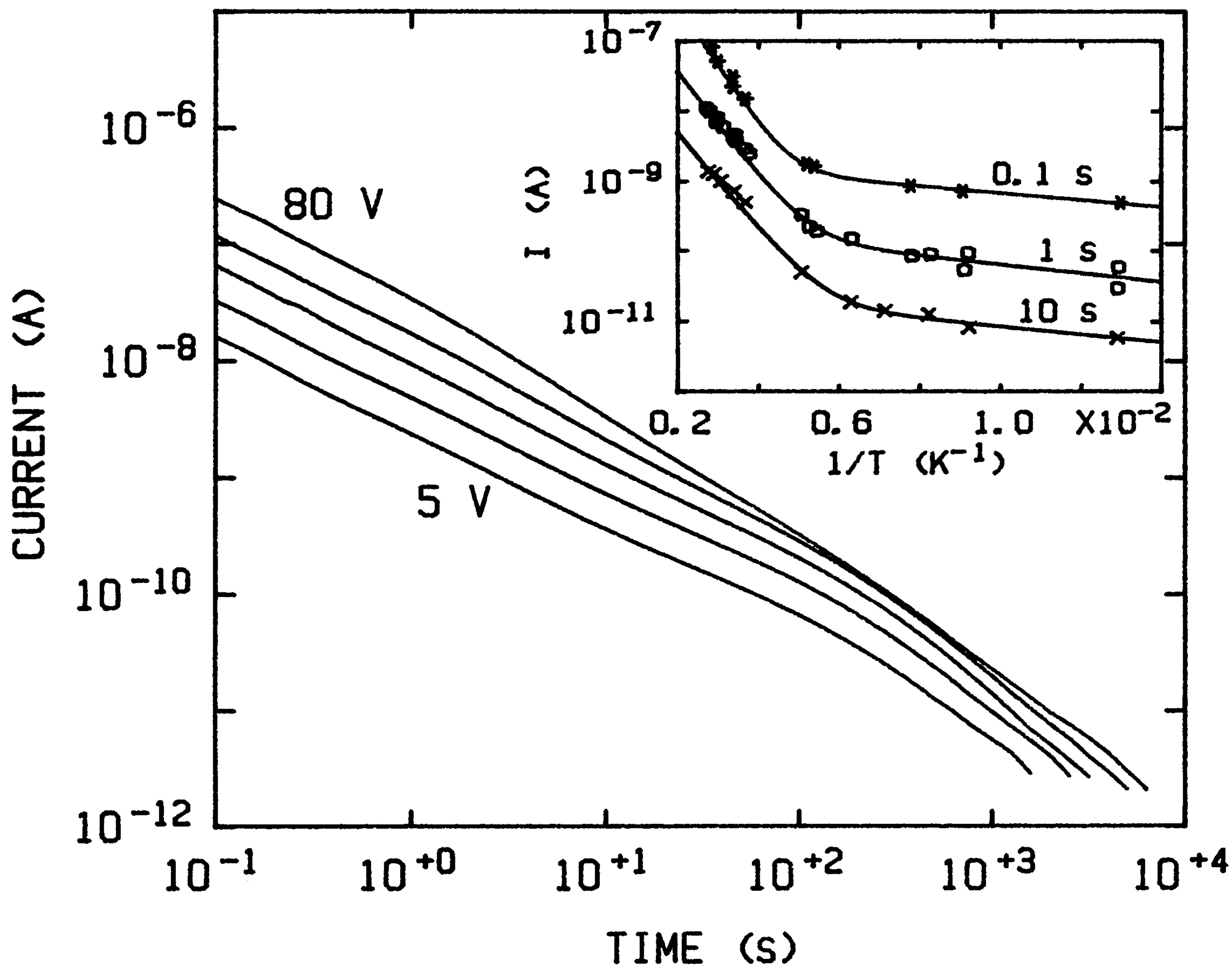

80 V
5 V
CURRENT (A)
TIME (s)
10^{-6}
10^{-8}
10^{-10}
10^{-12}
10^{-1}
10^{+0}
10^{+1}
10^{+2}
10^{+3}
10^{+4}
I (A)
1/T (K^{-1})
0.1 s
1 s
10 s
10^{-7}
10^{-9}
10^{-11}
0.2
0.6
1.0
X10^{-2}

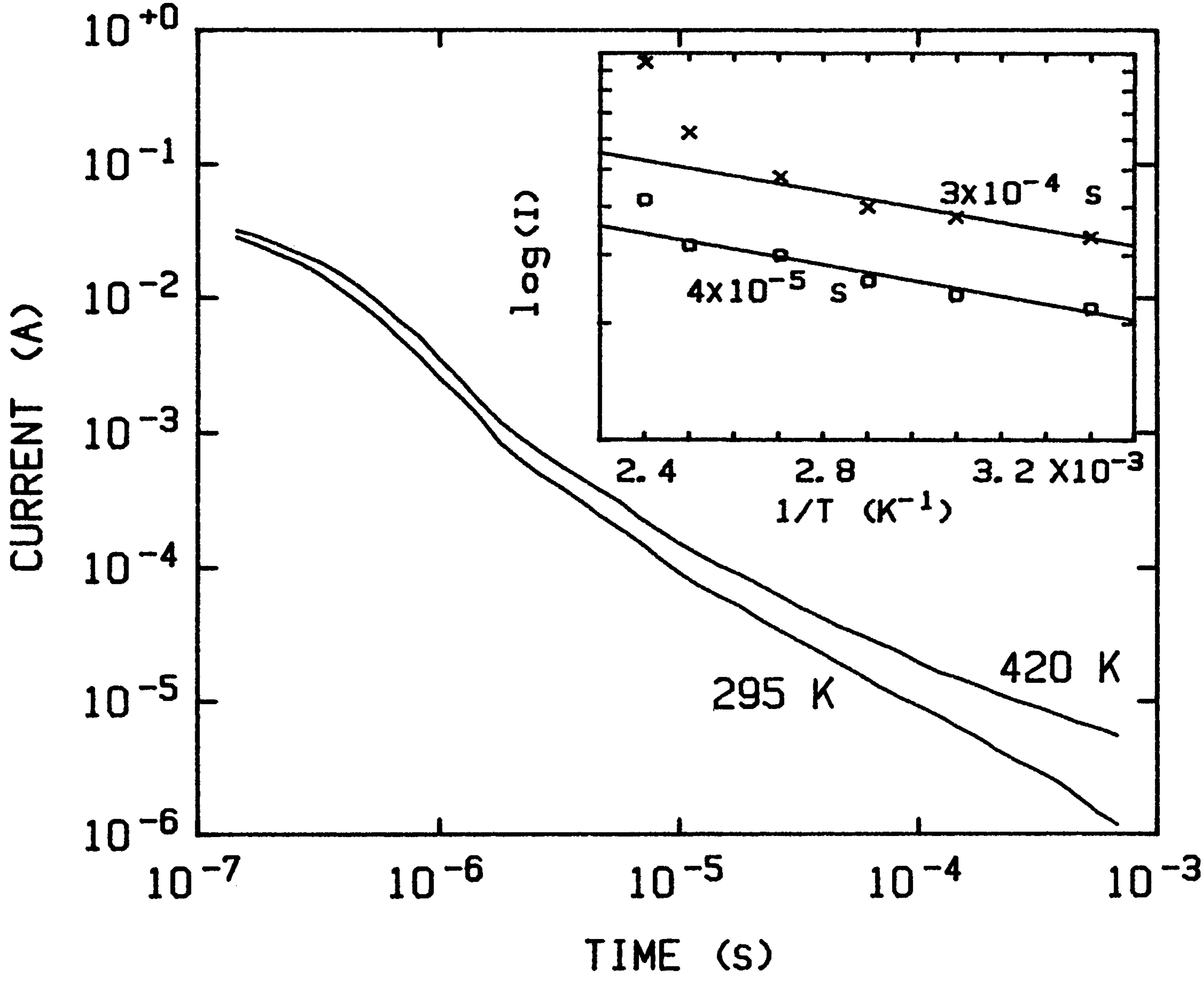
10 +0
10 −1
10 −2
10 −3
10 −4
10 −5
10 −6
CURRENT (A)
10 −7
10 −6
10 −5
10 −4
10 −3
TIME (s)
295 K
420 K
log(I)
3X10 −4 s
4X10 −5 s
2.4
2.8
3.2 X10 −3
1/T (K −1)

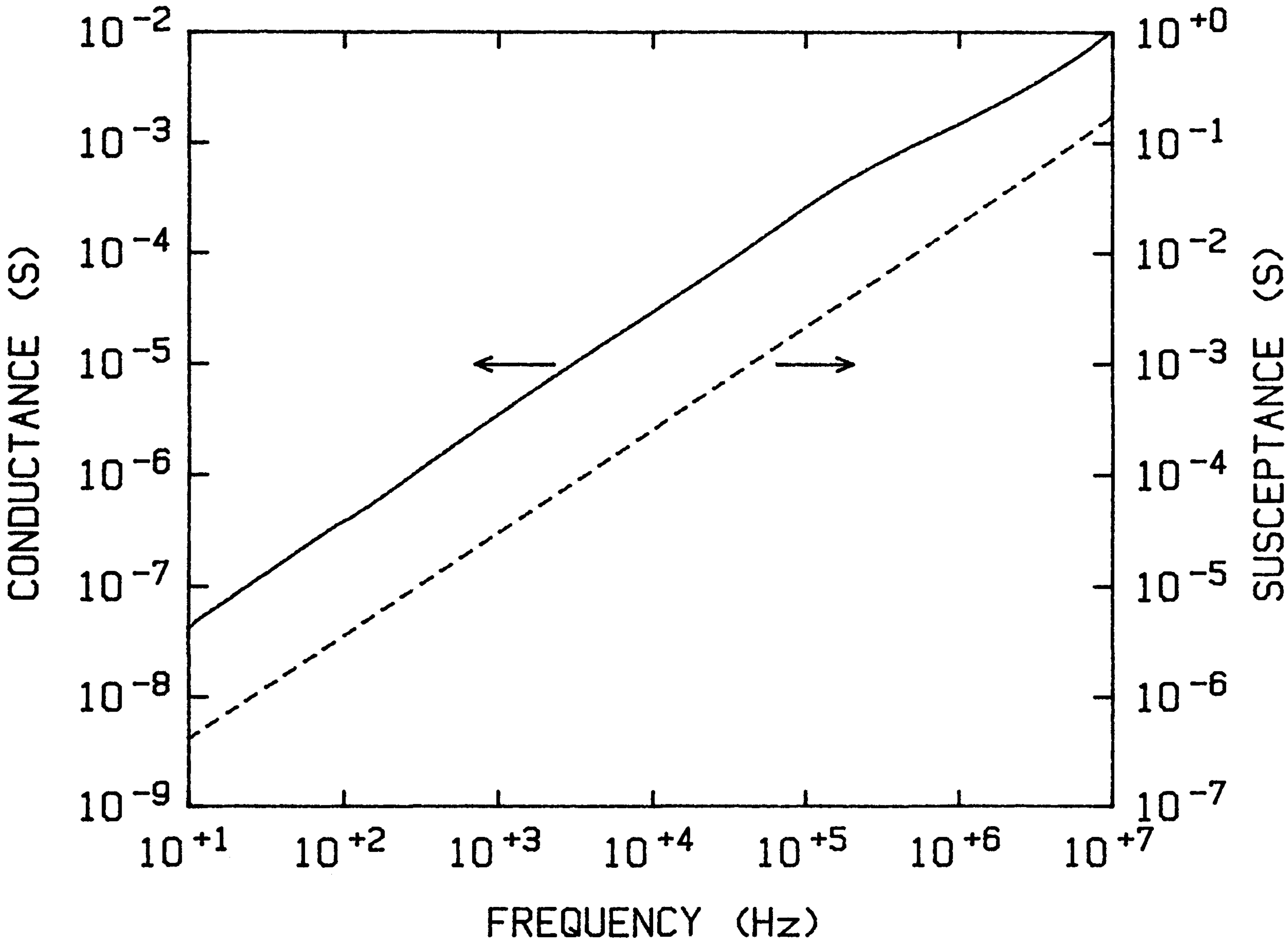

10 −2
10 −3
10 −4
10 −5
10 −6
10 −7
10 −8
10 −9
CONDUCTANCE (S)
10 +0
10 −1
10 −2
10 −3
10 −4
10 −5
10 −6
10 −7
SUSCEPTANCE (S)
10 +1
10 +2
10 +3
10 +4
10 +5
10 +6
10 +7
FREQUENCY (Hz)

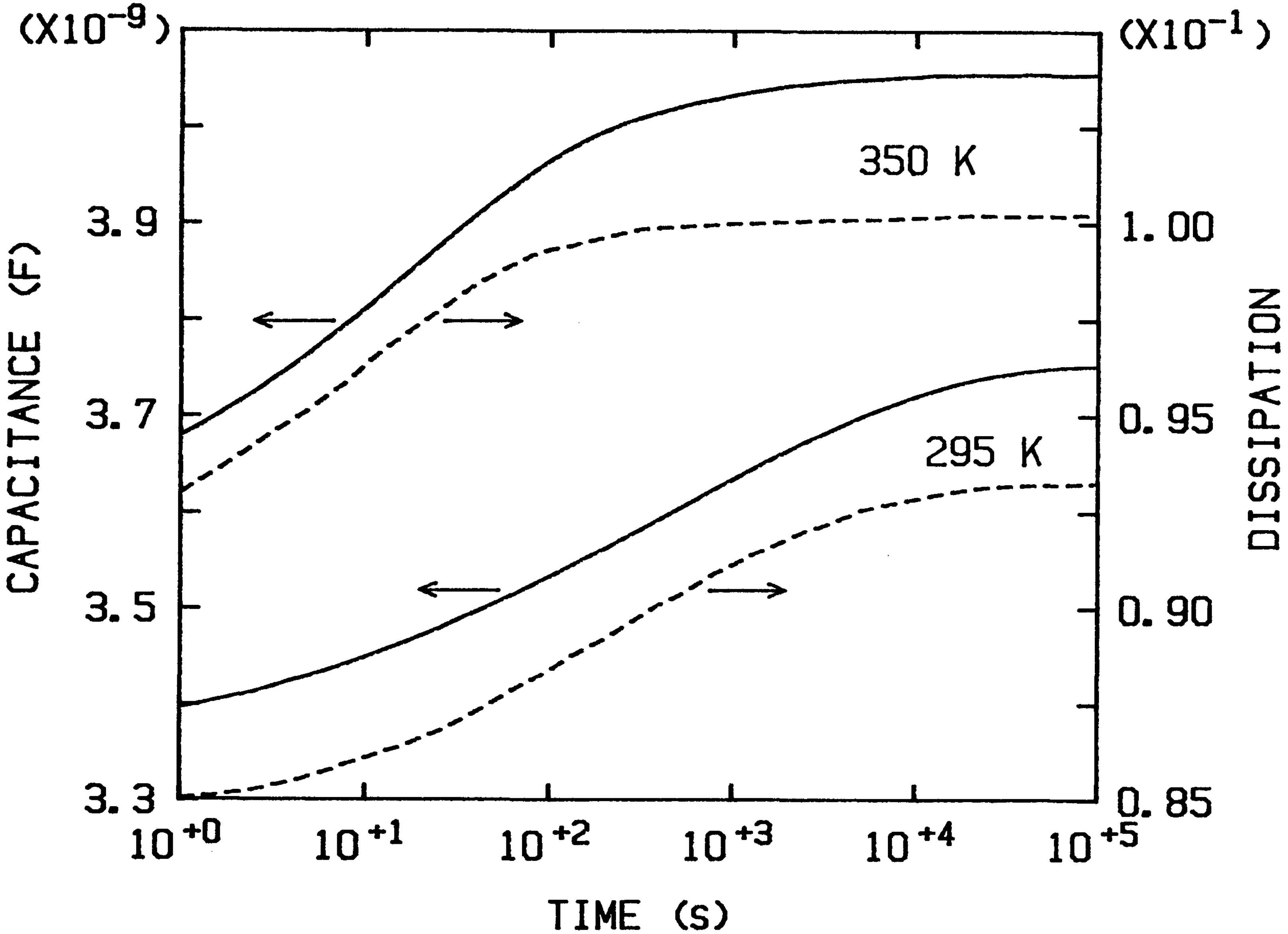

(X10^-9)
(X10^-1)
350 K
295 K
3.9
3.7
3.5
3.3
1.00
0.95
0.90
0.85
CAPACITANCE (F)
DISSIPATION
10^+0
10^+1
10^+2
10^+3
10^+4
10^+5
TIME (s)

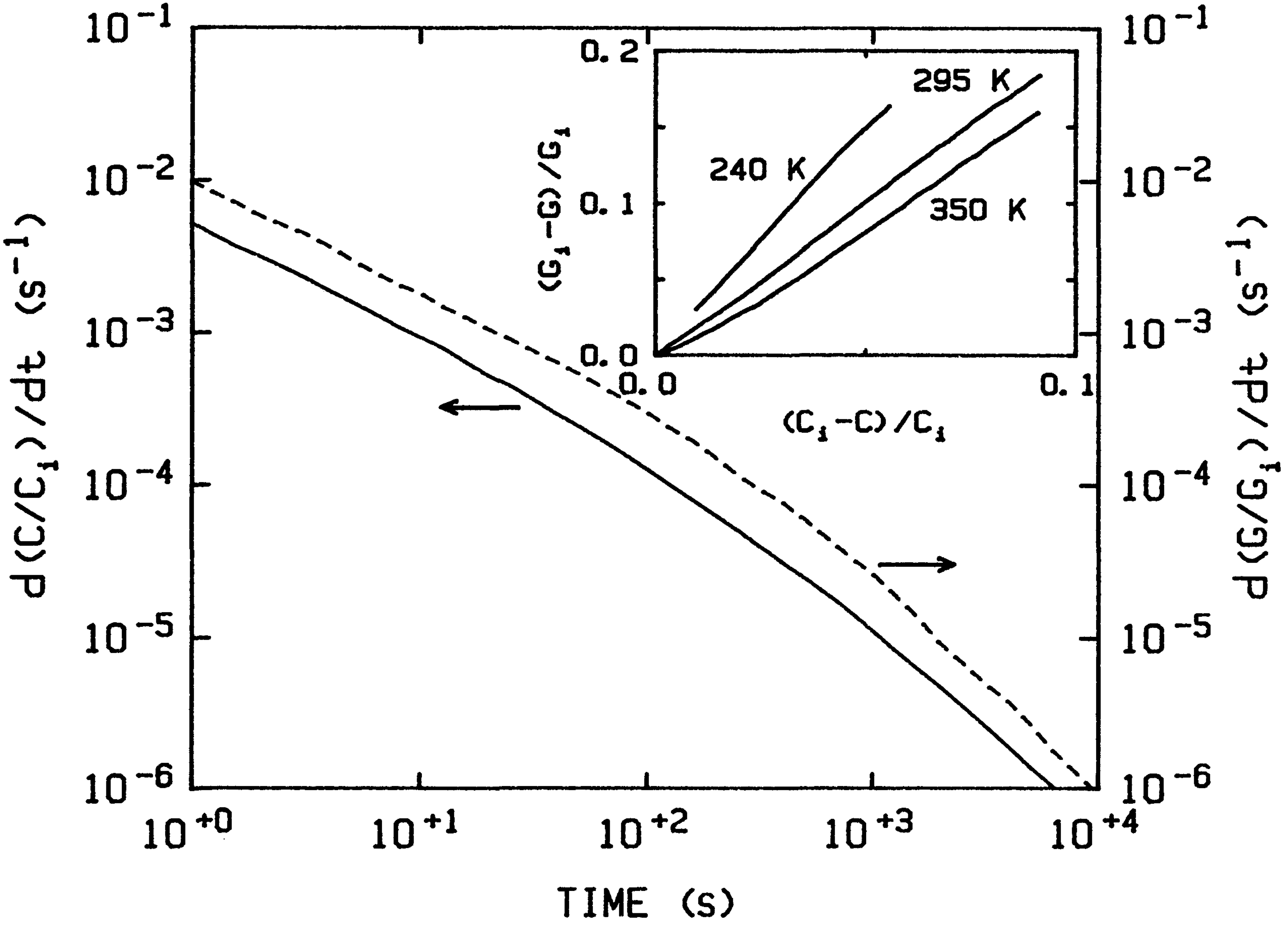

10^{-1}
10^{-2}
10^{-3}
10^{-4}
10^{-5}
10^{-6}
$d(C/C_i)/dt$ (s^{-1})
$d(G/G_i)/dt$ (s^{-1})
10^{+0}
10^{+1}
10^{+2}
10^{+3}
10^{+4}
TIME (s)
0.2
0.1
0.0
0.0
0.1
$(G_i-G)/G_i$
$(C_i-C)/C_i$
240 K
295 K
350 K